Available online at www.sciencedirect.com
SCIENCE DIRECT
Polymer 46 (2005) 903–914
polymer
www.elsevier.com/locate/polymer

Effect of clay modifier and matrix molar mass on the structure and properties of poly(ethylene oxide)/Cloisite nanocomposites via melt-compounding

Wendy Loyens, Patric Jannasch, Frans H.J. Maurer*

Department of Polymer Science and Engineering, Lund Institute of Technology, Lund University, P.O. Box 124, SE-221 00 Lund, Sweden

Received 21 June 2004; received in revised form 7 November 2004; accepted 22 November 2004
Available online 19 December 2004

Abstract

The present study is concerned with the preparation and characterisation of PEO/clay nanocomposites via melt-extrusion. Two different matrix molar masses of PEO were investigated as well as various types of the Cloisite clay range. PEO/Cloisite Na^+ nanocomposites give rise to intercalated structures displaying only a moderate improvement of the mechanical properties at higher clay concentrations, regardless of the matrix molar mass. The chemical nature of the organic modifier was proven to be detrimental for the final nanocomposite structure and resulting mechanical properties. PEO nanocomposites based on the Cloisite 30B clay, incorporating a polar modifier, give rise to exfoliated structures. They display a strongly increased storage modulus, regardless of the matrix molar mass. The structural organisation of the nanocomposites based on Cloisite 20A, containing an apolar modifier, is very dependent on the matrix molar mass. An exfoliated structure can only be achieved upon melt mixing with a high molar mass PEO. In general, the mechanical properties of the nanocomposites based on the high molar mass PEO matrix are slightly superior. The thermal properties are also distinctly influenced by the addition of clay, although the actual structural organisation of the nanocomposite is proven to be less important. The melt temperature, as well as the crystallinity, decreases upon the addition of clay, especially for the low molar mass PEO matrix. The decomposition temperature shows a slight increase upon the addition of clay, especially for the Cloisite 30B nanocomposites.

Keywords: Clay nanocomposites; PEO; SAXS

1. Introduction

Poly(ethylene oxide) (PEO)/clay nanocomposites are promising materials showing great potential for various applications. The addition of only a few weight percentages of clay is known to be very effective in providing materials with an interesting array of properties [1,2]. The formation of intercalated, or even exfoliated nanostructures, generally leads to highly improved mechanical properties (modulus and strength), altered thermal characteristics, as well as a decreased gas permeability and improved flame retardancy [2–4].

Research efforts on PEO/clay nanocomposites have mainly originated from the area of polymer electrolytes [5–12], wherein PEO/salt complexes form one of the most extensively studied systems. Efforts have been largely limited to the investigation of PEO nanocomposites based on natural montmorillonite, containing either Na^+ ions or ion-exchanged Li^+ in the intergallery spacing [6,12–16]. PEO has been found to be able to intercalate in the intergallery spacing of the clay giving rise to a limited increase of the basal spacing (7–8 Å). Many studies have furthermore focussed on the conformation of the PEO chains in between the silicate clay layers. However, contradicting results have been presented, as several authors reported on the existence of a helical PEO crystal structure [6,14], whereas others consider a double PEO chain layer without any crystal formation [15].

Many of the investigated PEO/clay nanocomposites are composed of an excess (>50 wt%) concentration of clay. Hence, PEO actually forms the minor component of the

* Corresponding author. Tel.: +46 46 222 9149; fax: +46 46 222 4115.
E-mail address: frans.maurer@polymer.lth.se (F.H.J. Maurer).

0032-3861/$ - see front matter © 2004 Elsevier Ltd. All rights reserved.
doi:10.1016/j.polymer.2004.11.077

composite. In the literature, PEO/clay nanocomposites are most commonly prepared using solution [6,8,9,17] or steady-state annealing [10–12] processes. Melt extrusion, however, is a more convenient and industrially interesting route of preparation. It has been shown for polyamide/clay nanocomposites that a careful selection of the melt extrusion processing conditions and of the chemical compatibility between the matrix and the added clay provides a good means of creating a variety of nanocomposite structures [18].

The present paper is the first in a series of papers concerned with an extensive study of PEO/clay nanocomposites containing a low silicate content ($\leq$5.0 wt%) and prepared via melt-extrusion. This paper will focus on the investigation of the effect of the clay type, or more particularly the chemical nature of the organic modifier in the intergallery spacing, the clay concentration and the matrix molar mass. Three different clay types belonging to the commercially available Cloisite® clay range, are studied. Besides the natural montmorillonite clay containing Na^+ ions in the intergallery spacing (Cloisite Na^+), two different organically modified clays will be investigated. They include an apolar (Cloisite 20A) and a polar (Cloisite 30B) modifier, respectively. All nanocomposites are prepared and characterised for two different molar mass PEO matrices. The structural organisation, the mechanical and thermal properties of the various nanocomposites will be explored. The study intends to provide a good insight of the main parameters which can be manipulated in order to control the nanocomposite structure and thus the resulting properties of PEO/clay nanocomposites.

2. Experimental

2.1. Materials

Two commercial grades of PEO, with a respective molar mass of 100,000 g/mol (LMW) and 300,000 g/mol (HMW), were purchased from Aldrich. The examined clay types were purchased from Southern Clay Products. Cloisite Na^+ is the pure, non-modified form of the montmorillonite clay (MMT-Na^+). Cloisite 20A is organically modified with dimethyl dihydrogenated tallow quaternary ammonium (MMT-20A), while Cloisite 30B is organically modified with methyl tallow bis-2-hydroxyethyl quaternary ammonium cations (MMT-30B). The PEO grades and the clays were dried before use.

2.2. Melt-compounding

The nanocomposites were prepared in a two-step melt-compounding procedure. Their composition is based on the effective weight percentage of the clay silicate, providing a modifier independent basis for comparison. Firstly, a 10 wt% PEO/silicate masterbatch was compounded using a Brabender batch mixer at 120 °C, 40 rpm during 8 min. In the second compounding step, the masterbatch was diluted with neat PEO using a co-rotating twin screw midi-extruder at 120 °C (150 °C for HMW PEO), 80 rpm during 10 min. The use of a recirculation channel allows the extruder to be operated as a batch mixer. The silicate content was varied between 0 and 2.5 wt%. The nanocomposites based on the LMW PEO were also prepared with a silicate content of 5.0 wt%. After melt mixing, the nanocomposites were compression moulded into 1 mm thick samples at 120 °C and left to cool to room temperature. Before characterisation, the samples are dried overnight at 40 °C and kept in a dessicator until the measurements.

2.3. Small angle X-ray scattering (SAXS)

Structural information is gathered from SAXS experiments. They were performed on a Kratky compact camera equipped with a linear position sensitive detector (OED 50M from MBraun, Graz). A Seifert ID 3000 X-ray generator provides the Cu K_α radiation with a wavelength of 1.542 Å. The samples were placed in a sealed solid sample cell between mica sheets and measured during 1 h at 25 °C.

2.4. Dynamic mechanical properties (Torsion pendulum)

The dynamic mechanical properties in shear were determined using a torsion pendulum ATM3 Myrenne apparatus. The experiments were performed in the temperature range −90–30 °C at a heating rate of 2 °C/min and a frequency of 1 Hz. The samples had a thickness of 1 mm, a width of 9 mm and a measuring length of 50 mm.

2.5. Differential scanning calorimetry (DSC)

Differential scanning calorimetric measurements were performed on a TA Instruments Q1000 DSC. A first heating run was conducted from room temperature to 120 °C, followed by a cooling run down to −70 °C. The second heating run was performed from −70 to 120 °C. The heating/cooling rate was 10 °C/min.

2.6. Thermogravimetric analysis (TGA)

Determination of the thermal stability of the materials was performed on a TA Instruments Q500 TGA. The measurements were conducted from 40 to 900 °C at a heating rate of 10 °C/min under a N_2-flow.

3. Results and discussion

3.1. Structural organisation

In order to evaluate the extent of intercalation/exfoliation

of the added clay platelets upon melt mixing, SAXS measurements were performed and the results are depicted in Figs. 1(a)–(c) and 2(a)–(c) for the LMW and HMW PEO nanocomposites, respectively. Table 1 summarises the basal spacing for the pure clays and the respective nanocomposites for both molar mass PEO matrices. It immediately becomes clear that various parameters have a strong influence on the final nanocomposite structure.

Firstly, the LMW PEO nanocomposites will be considered. Fig. 1(a) presents the diffraction spectra of the Cloisite Na^+ based composites. The basal spacing of the pure Cloisite Na^+ clay is situated around 11.5 Å. This peak is not clearly visible from the present SAXS measurements due to the detection limit of the test equipment. The actual peak location was detected using more powerful SAXS equipment (result not shown). When melt mixed with PEO, a single diffraction peak becomes apparent around 18 Å. Hence, intercalated structures are formed upon melt mixing PEO and Cloisite Na^+ resulting in a basal spacing increase (Δd) of approximately 6.5 Å. This is in good agreement with previous reports in literature concerning PEO/Cloisite Na^+ nanocomposites, regardless of the method of preparation [5,13]. Pure Cloisite 20A has a basal spacing of 24.4 Å. Its respective LMW PEO nanocomposites show an increase of the basal spacing to around 37 Å ($\Delta d = 12.6$ Å) independent of the clay concentration, clearly indicating the intercalation of PEO (Fig. 1(b)). The SAXS spectra reveal the presence of a second small diffraction peak around 18 Å. This peak is located at a 2ϑ position which is exactly double the position of the main peak. Together with the obvious broadening of the primary diffraction peak, this indicates a high degree of ordering of the intercalated structure [19,20]. The pure Cloisite 30B clay shows a basal spacing of 18.6 Å (Fig. 1(c) and Table 1). Melt mixing with LMW PEO apparently leads to exfoliated nanocomposites, displaying no clear SAXS diffraction peaks. However, at higher silicate concentrations (≥ 2.5 wt%) a small peak can be seen, located at a similar position as the pure clay. This may indicate that there exists a threshold level for the clay concentration above which the amount of clay becomes too high in order to accomplish complete exfoliation.

Since the extrusion conditions for all examined nanocomposites are equal; the difference in the nanostructure formed can be primarily assigned to the difference in clay type, or more particularly, clay modifier. It becomes clear that a lack of organic modifier in the intergallery spacing of Cloisite Na^+ leads to the smallest increase of basal spacing. Hence, the use of an organic modifier appears essential whereby the specific chemical structure of the modifier is important. An increased compatibility between the modifier and the matrix can lead to exfoliated structures. This is clearly illustrated by the PEO/Cloisite 30B nanocomposites, as the clay contains a polar modifier. The apolar modifier in Cloisite 20A leads to an apparent lower compatibility, resulting in intercalated structures.

The nanocomposite structure formed also depends strongly on the matrix molar mass during melt mixing. The SAXS diffraction spectra of the HMW PEO nanocomposites are displayed in Fig. 2(a)–(c). The Cloisite Na^+ nanocomposites display a single diffraction peak around 18 Å, in close similarity to the results for the LMW PEO materials. The Cloisite 20A nanocomposites, however, reveal no diffraction peaks, providing a strong indication that a higher matrix molar mass gives rise to exfoliated clay platelets. The Cloisite 30B nanocomposites display no SAXS diffraction peaks, similar to their respective LMW PEO nanocomposites and thus indicating the formation of an exfoliated nanostructure. The influence of an increased matrix molar mass on the final nanocomposite structure is not surprising. Increasing the molar mass implies a simultaneous increase of the matrix melt viscosity, which accordingly leads to higher shear forces during melt mixing. This has been reported to be beneficial for the exfoliation process. In addition, the chemical compatibility between the polymer and the clay/organic modifier needs to be sufficiently high [18,21]. Hence, the reason for the formation of intercalated structures when adding Cloisite Na^+, regardless of the PEO molar mass.

3.2. Mechanical properties

The nanocomposite structure can have a vast influence on the mechanical properties, depending on the level of intercalation/exfoliation [1–3]. The dynamic mechanical characteristics were examined using a torsion pendulum apparatus, whereby an initial angular deformation is forced on the sample, and the resulting free damping vibration is monitored. Fig. 3(a) and (b) presents the shear storage

Table 1
Basal spacing of the PEO nanocomposites as a function of the matrix molar mass for the different clay types and silicate concentrations

Silicate concentration (wt%)	Cloisite Na^+		Cloisite 20A		Cloisite 30B	
	LMW	HMW	LMW	HMW	LMW	HMW
0	11.5	11.5	24.4	24.4	18.6	18.6
0.5	–[a]	–[a]	37.1	E[b]	E	E
1.0	17.7	18.5	37.0	E	E	E
2.5	18.3	18.6	37.2	E	(18)	E
5.0	17.9		36.8			

[a] –, not detectable by SAXS.
[b] E, exfoliated structure.

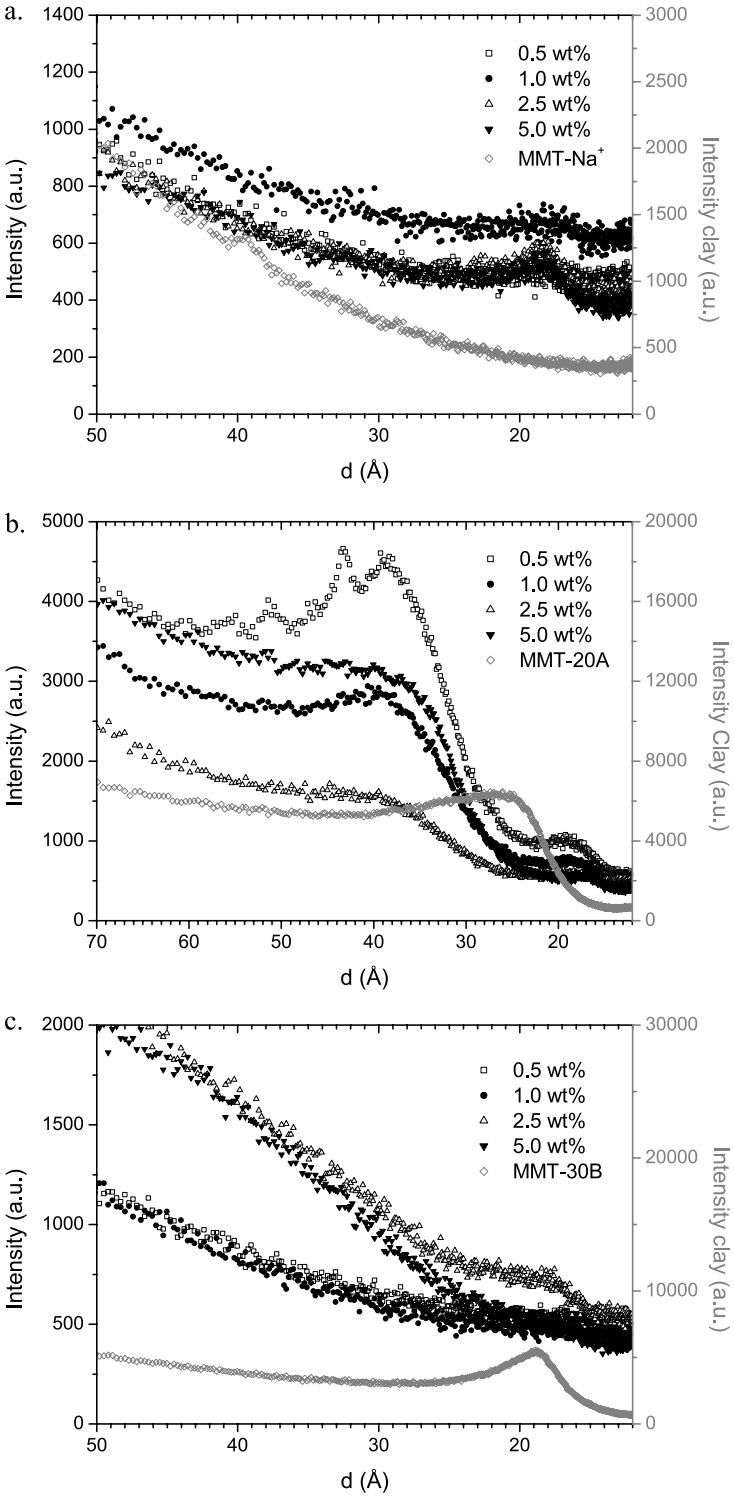

Fig. 1. SAXS diffraction spectra for the different clay nanocomposites based on the LMW PEO matrix for the various silicate concentrations: (a) Cloisite Na^+ (MMT-Na^+); (b) Cloisite 20A (MMT-20A) and (c) Cloisite 30B (MMT-30). The left *Y*-axis represents the intensity associated with the nanocomposites whereas the right *Y*-axis needs to be associated with the intensities of the respective pure clay.

moduli (G') of the different nanocomposites containing 2.5 wt% clay, for the LMW and HMW PEO matrix, respectively. The clay type is found to play a distinct role with regard to the elastic response of the nanocomposite. The behaviour of the Cloisite Na^+ composites is very comparable to that of the respective matrix material, whereas the nanocomposites based on the organically modified clays display distinctly higher shear storage moduli over the examined temperature range.

To evaluate the real contribution of the clay dispersion,

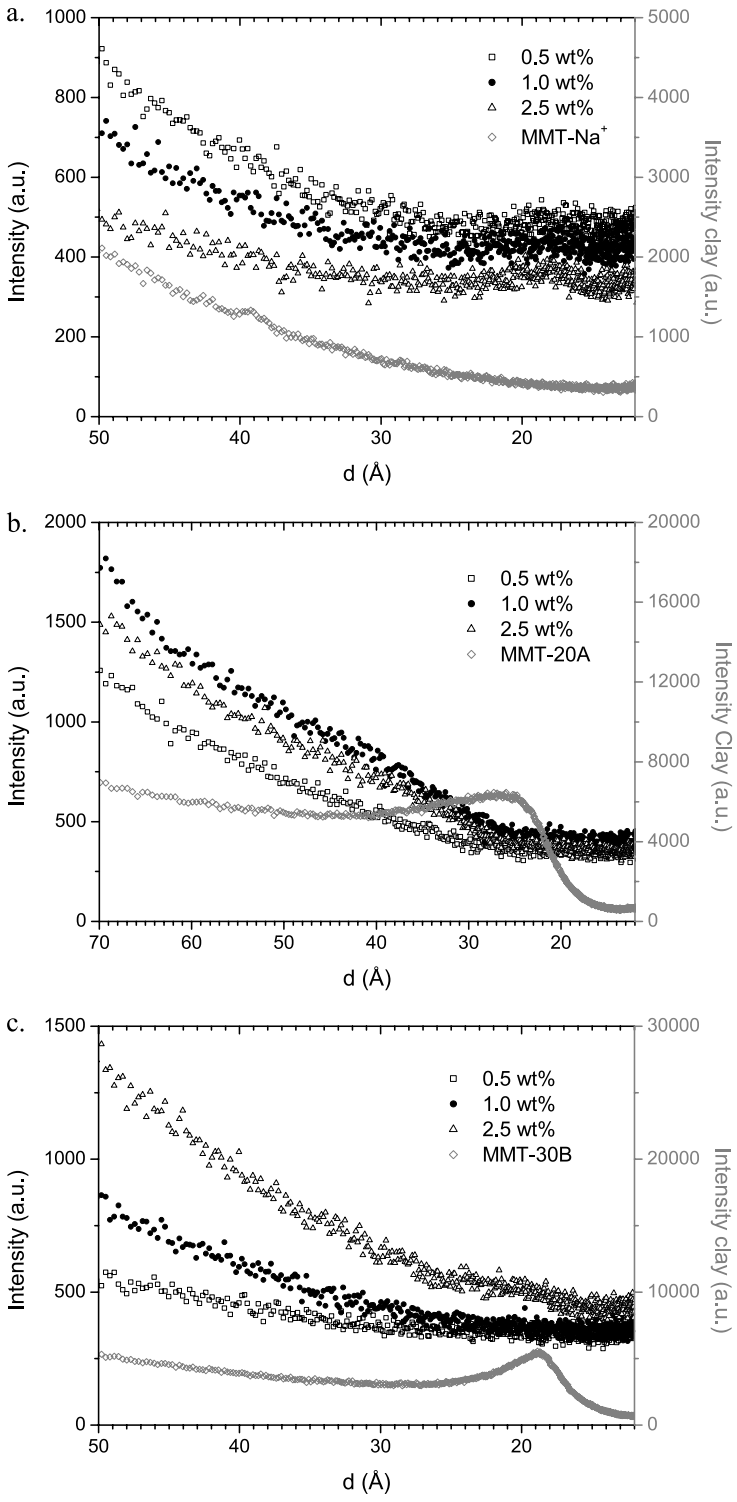

Fig. 2. SAXS diffraction spectra for the different clay nanocomposites based on the HMW PEO matrix for the various silicate concentrations: (a) Cloisite Na^+; (b) Cloisite 20A and (c) Cloisite 30B. The left *Y*-axis represents the intensity associated with the nanocomposites whereas the right *Y*-axis needs to be associated with the intensities of the respective pure clay.

the ratio between the shear storage modulus of the nanocomposite (G'_{nano}) and the shear storage modulus of the respective PEO matrix (G'_{PEO}) is evaluated. Tables 2 and 3 present the calculated ratios for the LMW and HMW PEO nanocomposites, respectively. At temperatures below the glass-transition temperature of the matrix (T_g), the dispersion of clay platelets has a minor influence on the storage modulus, regardless of the clay type. The addition of

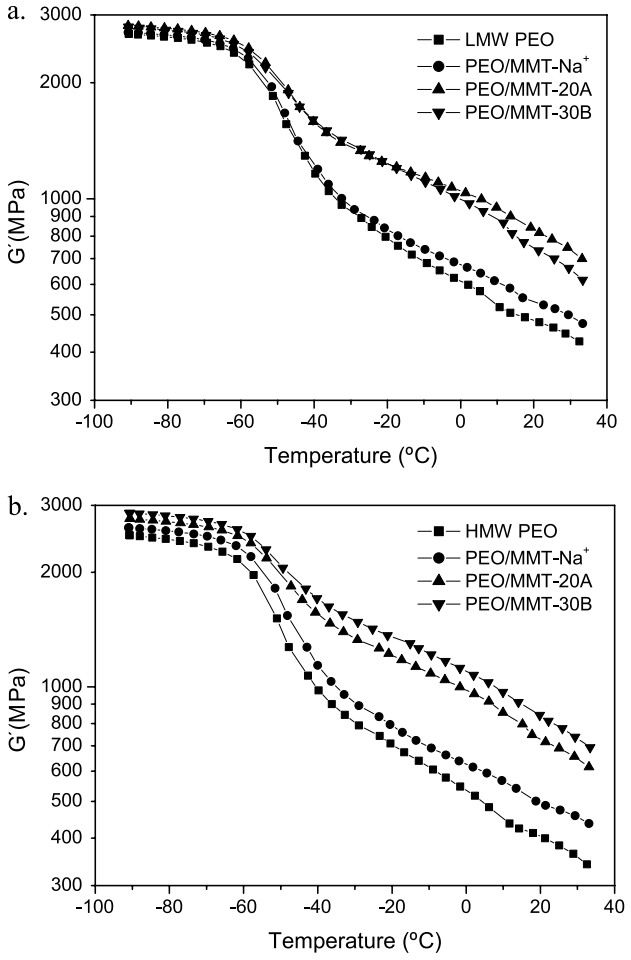

Fig. 3. The shear storage modulus (G') of the (a) LMW nanocomposites and the (b) HMW nanocomposites, containing 2.5 wt% silicate, as a function of the temperature for the different clay types.

Cloisite 30B is found to result in a slightly higher stiffening effect, for both molar mass PEO matrices. This is the result of a low relative modulus combined with a possible decrease of the matrix crystallinity in the presence of clays (see below), resulting in the apparent similarity of the respective storage moduli. At temperatures above the matrix T_g (e.g. 20 °C), the dispersion of clay can have a major stiffening effect (Tables 2 and 3 and Fig. 4(a)). The shear storage modulus is found to depend strongly on the clay

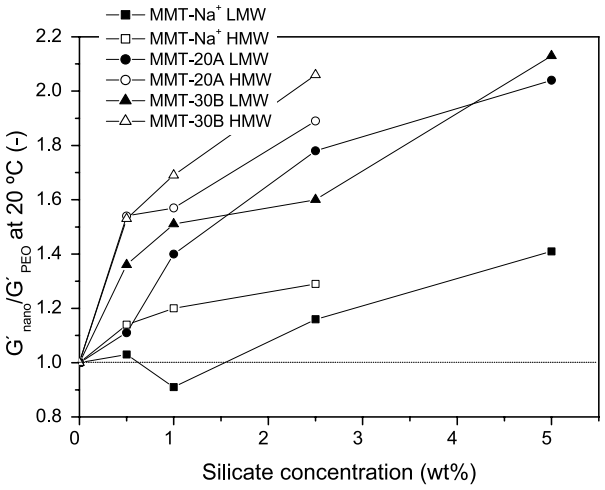

Fig. 4. Ratio between the shear storage modulus of the nanocomposite and the shear storage modulus of the respective PEO matrix (G'_{nano}/G'_{PEO}) as a function of the silicate concentration for the different clay types and matrix molar mass.

type, the formed nanocomposite structure, the silicate concentration and the matrix molar mass. The intercalated nanocomposites based on Cloisite Na^+ display no distinct improvement of the material stiffness, regardless of the matrix molar mass. Only at higher silicate concentrations ($\geq$5.0 wt%) a minor improvement can be observed. The LMW Cloisite 20A nanocomposites, forming intercalated structures with a relatively high interlayer spacing increase, reveal a gradual increase of the storage modulus with increasing silicate content. The exfoliated Cloisite 30B based LMW PEO nanocomposites reveal a superior stiffening effect, especially at lower silicate loadings. At higher concentrations, however, the possible presence of only partly exfoliated clay tactoids or even unintercalated platelets may lead to a decreased stiffening effect resulting from a decreased effective clay aspect ratio [2,3,21]. Using a modified version of the Halpin–Tsai model, the effective aspect ratio of the respective dispersed clay can be evaluated. The model has been corrected for platelet reinforcement [3]:

$$\frac{G_{nano}}{G_m} = \frac{1 + \xi\eta V_f}{1 - \eta V_f} \quad (1)$$

Table 2
Ratio between the shear storage modulus of the nanocomposite and the shear storage modulus of the LMW-PEO matrix (G'_{nano}/G'_{PEO}) as a function of the weight percentage of silicate for different clay types at −80 and 20 °C

Silicate concentration (wt%)	Cloisite Na^+		Cloisite 20A		Cloisite 30B	
	−80 °C	20 °C	−80 °C	20 °C	−80 °C	20 °C
0	1	1	1	1	1	1
0.5	1.05	1.03	0.96	1.11	1.06	1.35
1.0	1.01	0.91	1.07	1.4	1.05	1.50
2.5	1.05	1.16	1.09	1.78	1.08	1.6
5.0	1.12	1.41	1.17	2.04	1.24	2.13

Table 3
Ratio between the shear storage modulus of the nanocomposite and the shear storage modulus of the HMW-PEO matrix (G'_{nano}/G'_{PEO}) as a function of the weight percentage of silicate for the different clay types at −80 and 20 °C

Silicate concentration (wt%)	Cloisite Na^+		Cloisite 20A		Cloisite 30B	
	−80 °C	20 °C	−80 °C	20 °C	−80 °C	20 °C
0	1	1	1	1	1	1
0.5	1.05	1.14	1.07	1.54	1.04	1.53
1.0	1.11	1.20	1.06	1.57	1.10	1.69
2.5	1.09	1.29	1.15	1.89	1.20	2.06

with:

$$\eta = \frac{G_r/G_m - 1}{G_r/G_m + \xi} \quad (2)$$

$$\xi = \frac{w}{t} \quad (3)$$

G_{nano}, G_m and G_r are respectively the shear modulus of the nanocomposite, the matrix and the clay reinforcement. V_f is the volume concentration of the clay silicate and w/t is the aspect ratio of the added clay.

The shear modulus displays the distinct advantage of being independent of the distribution of the filler, in contrast to the elastic modulus [22]. Fig. 5 presents the fitting results for the different PEO/Cloisite nanocomposites as a function of the silicate volume concentration. Two aspect ratios were used as a fitting parameter. The supplier provides an aspect ratio (w/t) of 100 for these Cloisite clays. It becomes clear the fitted model offers clarification of the obtained mechanical properties. The PEO/Cloisite Na^+ nanocomposites display shear moduli far below the fitted values based on an aspect ratio of 100 and 50 (100/2), respectively. Only at a very low silicate concentration, an acceptable fit is obtained. These results clearly indicate that the effective aspect ratio of the dispersed silicate in the Cloisite Na^+ nanocomposites is very low. Van Es [3] reported previously that a high effective aspect ratio was crucial for polyamide/Cloisite 20A nanocomposites to reach a high elastic modulus. This is confirmed by the results presented in Fig. 5(b) and (c) for the nanocomposites based on Cloisite 20A and Cloisite 30B, respectively. The nanocomposites even display an underestimation of the fitted model at low silicate concentrations, whereas the experimental values become lower then the predicted ones at higher silicate concentrations ($\geq$2.5 wt%). The underestimation of the model can be caused by different factors. The model is based on the bulk modulus of the matrix material. However, it is not unlikely that the matrix around the platelets has a higher stiffness then in the bulk and as such also has a distinct contribution to the mechanical properties. On the other hand, the underestimation implies that the clay platelets are actually longer then originally believed. This can be explained by a percolation (overlapping) of the different platelets, leading to an apparent increase of the length and not necessarily of the thickness.

It becomes also obvious that the effective aspect ratio becomes lower with increasing clay volume concentrations. This effect is the clearest for the PEO/Cloisite 30B nanocomposites. Hence, there appears to exist a threshold level above which exfoliation is no longer complete. This supports the SAXS results which revealed the presence of a diffraction peak at the peak position of the pure clay at higher clay loadings (see Fig. 1(c)).

The HMW PEO nanocomposites based on Cloisite 20A and Cloisite 30B provide very interesting systems as both display apparent exfoliated structures (see Fig. 2(b) and (c)). At a low silicate concentrations their mechanical characteristics are basically identical. However, upon increasing the silicate content, the Cloisite 30B nanocomposites display a superior stiffening effect over the Cloisite 20A composites. From Fig. 4, it can be clearly concluded that the HMW PEO nanocomposites display a stronger stiffening effect over the respective LMW PEO nanocomposites. It is especially interesting to notice that the response of the Cloisite 30B nanocomposites (all exfoliated) seems to be highly influenced by the matrix molar mass. It has been reported before that a higher matrix molar mass, results in better mechanical properties [21]. When investigating the influence of the matrix molar mass on the mechanical properties, it is important to distinguish between two different physical effects. The molar mass influences both the melt viscosity, thus the nanocomposite structure formed and the matrix crystallinity. This will be addressed below.

Fig. 6(a)–(c) presents the tan δ values as a function of the temperature for the three LMW PEO clay nanocomposites. The onset of the PEO glass-transition region is significantly altered by the dispersion of clay platelets, regardless of the clay type. It can be seen that the onset of the glass-transition shifts towards higher temperatures with increasing silicate loading. The loss modulus (G'') response displayed a corresponding increase of the T_g with increasing silicate content ($\sim$5 °C). This effect can most probably be attributed to a slight restriction of the chain mobility of the PEO chains near the clay platelets. The HMW PEO nanocomposites display a similar response. A second transition at higher temperatures can be observed both for the pure PEO matrix as well as its respective nanocomposites. This transition is clearest for the LMW materials. A similar relaxation has been studied extensively for linear polyethylene and was assigned to the ability to form a mobile localised structure [23,24]. The energy of the formation of this entity should be

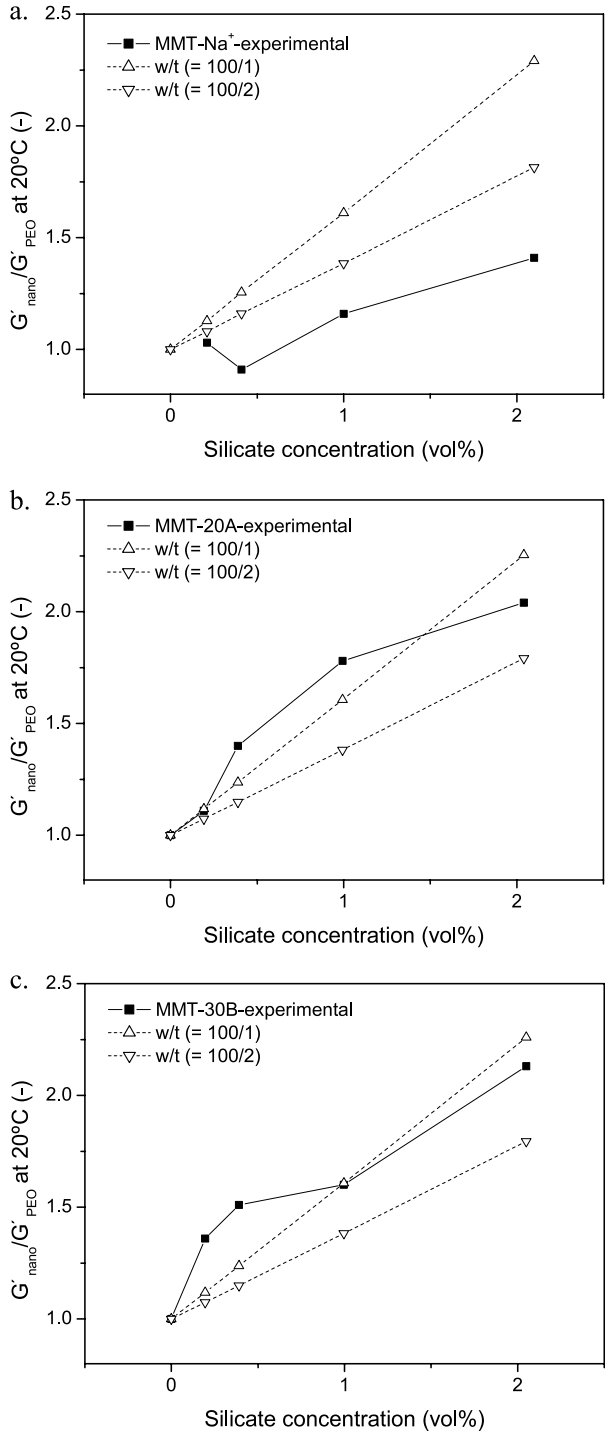

Fig. 5. Ratio between the shear storage modulus of the nanocomposite and the shear storage modulus of the LMW PEO matrix (G'_{nano}/G'_{PEO}) as a function of the silicate volume concentration (closed symbols) for Cloisite Na^+ (a); Cloisite 20A (b) and Cloisite 30B (c). The open symbols represent the respective (G'_{nano}/G'_{PEO}) value as predicted by the modified Halpin Tsai model for two different aspect ratios (100/1 and 100/2).

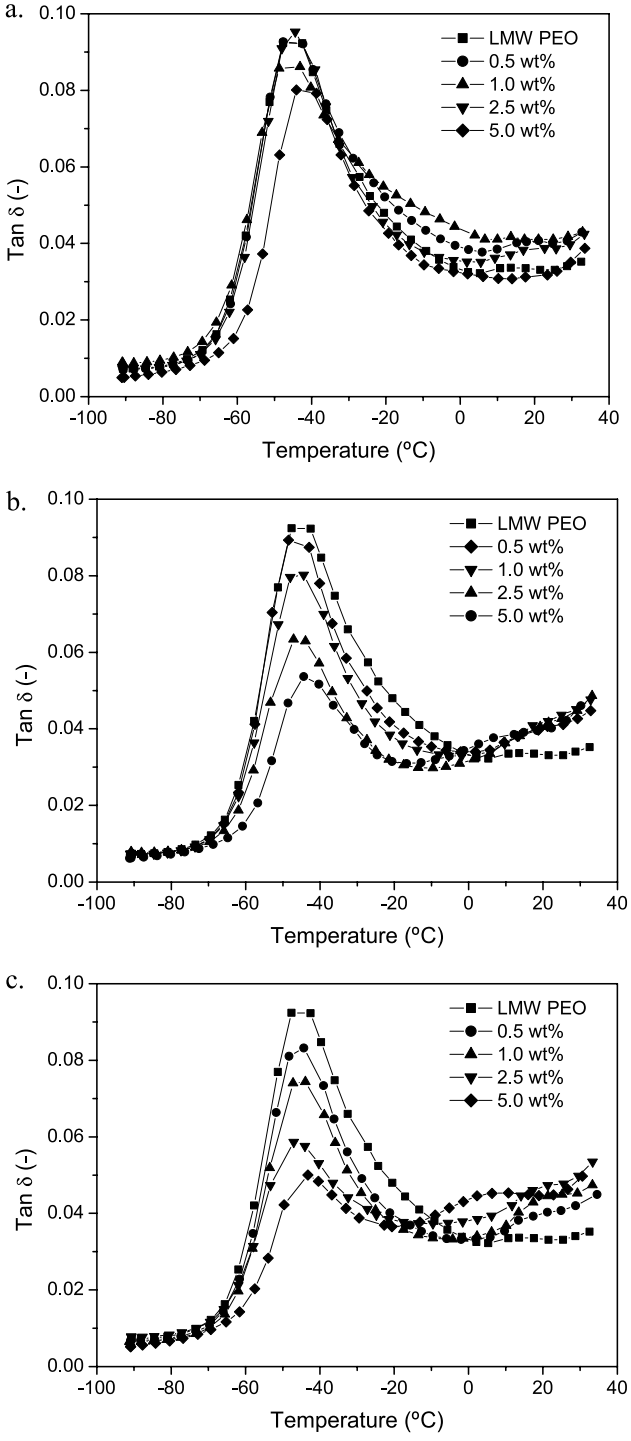

Fig. 6. Tan δ response as a function of temperature for the different LMW nanocomposites: (a) Cloisite Na^+; (b) Cloisite 20A and (c) Cloisite 30B, for the various silicate concentrations.

low enough to provide correspondingly low relaxation times in order to give rise to an observable process below the melting point. PEO has a similar flexibility compared to PE and is thus reported to be liable for this kind of processes [24]. The mechanically observable process requires the presence of the crystal phase, but its relaxation strength is assigned to the amorphous component and involves softening or deformation of this phase [23].

It is very interesting to note that the tan δ value at the peak position provides an indication of the level of clay

Table 4
Thermal characteristics determined via DSC measurements of the different LMW PEO nanocomposites as a function of the silicate concentration

Silicate concentration (wt%)	First heating		Cooling, $T_{c,onset}$ (°C)	Second heating	
	ΔH_{m1} (J/g PEO)	$T_{m1,onset}$ (°C)		ΔH_{m2} (J/g PEO)	$T_{m2,onset}$ (°C)
LMW PEO	168.5±3.0	59.8±1.2	52.0±0.2	161.6±3.6	58.3±2.3
Cloisite Na^+					
0.5	164.5	59.0	51.4	149.9	59.0
1.0	163.5	58.4	51.8	151.3	58.4
2.5	166.2	59.6	52.3	153.9	59.6
5.0	167.7	61.5	52.0	158.4	57.2
Cloisite 20A					
0.5	162.3	59.4	52.0	150.5	57.1
1.0	162.9	57.9	51.8	152.5	56.7
2.5	163.2	58.1	51.0	148.6	54.1
5.0	162.2	60.0	50.7	159.6	57.4
Cloisite 30B					
0.5	160.0	58.1	51.5	151.1	54.2
1.0	163.3	60.4	52.1	153.4	57.1
2.5	158.5	58.7	50.8	149.8	53.3
5.0	166.1	61.1	51.0	158.9	58.4

dispersion. The peak level is clearly found to decrease for the highly intercalated (Cloisite 20A) and exfoliated (Cloisite 30B) nanocomposites. In general, the HMW nanocomposites reveal a similar behaviour, displaying slightly lower T_g's as a result of the lower T_g of the HMW matrix PEO.

3.3. Crystallisation characteristics

The addition of clay to a semi-crystalline polymer is not unlikely to result in some distinct changes of the thermal characteristics. The crystallisation and melting behaviour of the various PEO/clay nanocomposites has been evaluated with DSC. The thermal characteristics are presented in Tables 4 and 5 for the LMW and HMW PEO nanocomposites, respectively. As expected, the dispersion of clay platelets can have a significant effect on the crystallisation behaviour of PEO. The Cloisite Na^+ LMW PEO nanocomposites display crystallisation temperatures (T_c) which are highly comparable to the one of pure PEO. The nanocomposites based on the organically modified clays also display T_c's which are similar to the one of pure PEO at low clay concentrations. However, the T_c is found to decrease at higher clay loadings ($\geq$2.5 wt%). The HMW PEO materials display an analogous evolution of T_c, whereby the values of the Cloisite Na^+ nanocomposites are positioned at slightly higher temperatures. When comparing the respective LMW and HMW nanocomposites, it is evident that the HMW materials crystallise at lower temperatures. This is a consequence of the lower chain mobility of the HMW matrix, resulting in the need for a higher degree of undercooling to initiate crystallisation. Although it has been stated that the addition of clay has a nucleating effect [4,13], this is not apparent from the T_c values of our nanocomposites. In contrast, the decreased T_c's indicate that the crystallisation is delayed in the presence of higher clay loadings as a larger degree of undercooling is needed. The decrease of T_c with the addition

Table 5
Thermal characteristics determined via DSC measurements of the different HMW PEO nanocomposites as a function of the silicate concentration

Silicate concentration (wt%)	First heating		Cooling, $T_{c,onset}$ (°C)	Second heating	
	ΔH_{m1} (J/g PEO)	$T_{m1,onset}$ (°C)		ΔH_{m2} (J/g PEO)	$T_{m2,onset}$ (°C)
HMW PEO	154.7±1.6	61.1±3.0	47.6±0.7	147.4±1.6	53.7±1.2
Cloisite Na^+					
0.5	160.9	58.0	48.6	153.4	54.7
1.0	160.1	56.8	48.3	153.8	54.6
2.5	156.6	56.9	48.8	147.2	53.6
Cloisite 20A					
0.5	159.0	56.9	48.7	147.6	52.8
1.0	156.7	56.9	48.0	149.0	53.0
2.5	154.5	55.9	47.3	145.8	53.4
Cloisite 30B					
0.5	159.7	55.8	47.6	149.0	52.6
1.0	158.9	56.9	46.9	147.5	51.8
2.5	154.2	56.4	46.4	145.0	53.8

of clay has been reported before for PEO [13] and other [3,4] polymeric nanocomposites.

The heat of fusion derived from the PEO melting endotherm, obtained from both the first and the second heating run, reveals a strong influence of the clay addition. For the LMW materials, the addition of a low amount of clay (0.5 wt%) is sufficient to result in a distinct decrease of the melt enthalpy and thus crystallinity. Increasing the clay concentration appears not to have a strong effect, as the values remain approximately the same. However, the nanocomposites having a silicate concentration of 5.0 wt%, show a sudden sharp increase of the melt enthalpy to result in crystallinity levels comparable to the one of the LMW PEO matrix. The observed trend appears to be independent of the clay type, and thus the nanocomposite structure and chemical nature of the modifier. The PEO melt temperature of the LMW nanocomposites (T_m) displays a similar trend as its corresponding melt enthalpy. The T_m's of the Cloisite Na^+ materials are actually comparable to the one of PEO, whereas the organically modified clay nanocomposites reveal decreased melt temperatures upon the addition of clay. For a clay concentration of 5.0 wt%, an increase of T_m is observed, in close similarity to the evolution of the melt enthalpy. The decrease in melt enthalpy and respective melt temperature has been reported before for PEO nanocomposites [13,25], as well as for other polymer composites [3,4]. The HMW PEO nanocomposites display a slightly different behaviour for the heat of fusion.

Fig. 7 provides a comparative graph presenting the heat of fusion evaluated from the second heating run as a function of the clay concentration for both the LMW and the HMW PEO nanocomposites. In contrast to the LMW materials, the addition of a small amount of clay does not have a strong effect on the heat of fusion. Only the Cloisite Na^+ nanocomposites display an increased crystallinity for the lowest clay concentrations. Increasing the clay content leads to a decrease of the heat of fusion. The melting

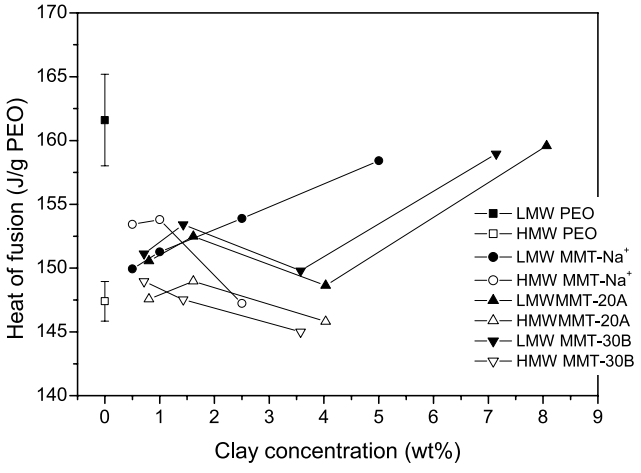

Fig. 7. Normalised heat of fusion, derived from the second heating DSC run, as a function of the clay (silicate and modifier) concentration for the various clay types and PEO molar mass.

temperatures of the HMW PEO nanocomposites are found to be comparable to the T_m of pure PEO, showing a slight decrease with increasing clay concentration. In general, it can be stated that both the degree of crystallinity and the melt temperature of the LMW PEO nanocomposites are clearly higher than the respective HMW PEO material. This is a direct consequence of the lower chain mobility of the HMW PEO [4]. The addition of clay is found to have a more profound effect on the thermal properties of the LMW PEO nanocomposites.

These DSC results lead to the conclusion that the addition of clay has an inhibiting effect on the crystallisation of the PEO matrix. It has been previously observed [4,13] that the presence of the dispersed clay platelets disturbs the crystal growth. The inhibition was explained by a restriction in chain mobility due to the limited amount of space available, thereby hindering part of the polymer chain from entering the crystalline structure. This results in smaller spherulites [13] and more disrupted, less perfect crystalline lamellae which is clearly reflected in the observed decreased melt temperatures. It seems that the hindrance is by no means directly related, or proportional, to the incorporation of the chain in the intergallery structure, as no distinct difference in the crystallisation behaviour between the intercalated (LMW Cloisite 20A) and the exfoliated (LMW Cloisite 30B) nanocomposites can be observed. The influence on the crystallisation characteristics of the entity in the intergallery spacing is not straightforward, although it may be stated that the Cloisite Na^+ nanocomposites display thermal properties closely related to those of PEO. The hindrance of the crystallisation in the presence of this natural clay can possibly be attributed to the presence of Na^+. From work on polymer electrolytes it is known that the presence of small cationic species has an inhibiting effect on the crystallisation of PEO as the polymer chain co-ordinates the cations which usually lowers the overall degree of crystallisation [13,26]. On the other hand, it is not unlikely that the presence of the bulky quaternary ammonium cations screens the clay surface, prohibiting crystalline nucleation.

The reason for the increase of the melt enthalpy at the high clay loading for the LMW PEO nanocomposites remains unclear, albeit interesting that a corresponding increase of the melt temperature is observed. This is a direct consequence of a higher lamellar thickness, thus the formation of more perfectly organised spherulites which can result in an increase of the overall degree of crystallisation. As mentioned above during the discussion of the nanocomposite structure (see Fig. 5), there appears to exist a threshold level (~2.5 wt%) above which the clay concentrations becomes too high for complete exfoliation to occur. As a consequence, the platelets remain present in more ordered stacks (Cloisite 20A) or even unintercalated tactoids (Cloisite 30B) (Fig. 1(b) and (c)), causing possibly less hindrance of the crystallisation process.

When correlating the mechanical properties and the

crystallisation characteristics of the respective nanocomposites (LMW: Tables 2 and 4; HMW: Tables 3 and 5), it becomes clear that no direct relationship between the level of crystallinity and the storage modulus can be found. This shows that the stiffening effect observed upon the addition of clay can be completely attributed to the consecutive formation of the intercalated or exfoliated nanocomposite structure.

3.4. Thermal stability

The effect of the addition of clay on the thermal stability was studied by TGA under N_2 flow. Fig. 8 shows the weight loss as a function of temperature for the different LMW PEO/clay nanocomposites, having a silicate concentration of 2.5 wt%. Fig. 9 presents the onset decomposition temperature as derived from the TGA experiments as a function of the silicate concentration. From both figures it can be seen that the addition has a beneficial effect on the thermal stability. The temperature for onset of thermal decomposition shows a clear increase at silicate concentrations as low as 0.5 wt%, especially for the Cloisite Na^+ nanocomposites. However, further increasing the Cloisite Na^+ content induces a decrease of the decomposition temperature. In contrast, the organically modified clay nanocomposites show an overall trend of increasing decomposition temperatures with silicate concentration. The difference between an exfoliated (Cloisite 30B) and an intercalated (Cloisite 20A) nanostructure is minimised at high silicate contents. As mentioned above, the observed threshold level for silicate content indicates that not all clay platelets are fully exfoliated, causing the effective aspect ratio to be lowered. Accordingly, this material is more likely to display characteristics of intercalated structures [2]. In addition, it is not unlikely that the nanocomposite morphology at the elevated temperatures in quiescent conditions changes from the one observed at ambient

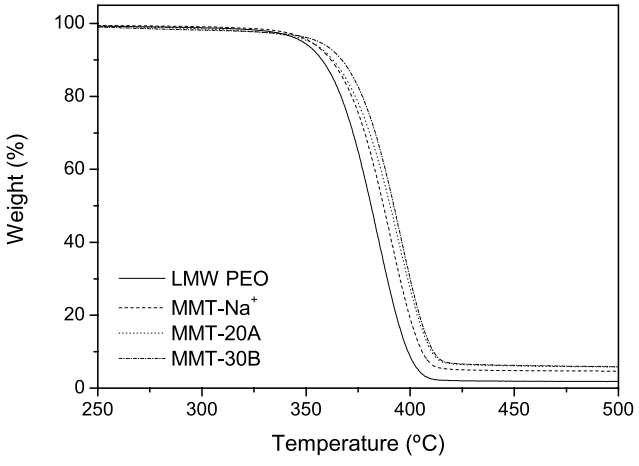

Fig. 8. TGA response of the pure LMW PEO and its different clay nanocomposites containing 2.5 wt% silicate.

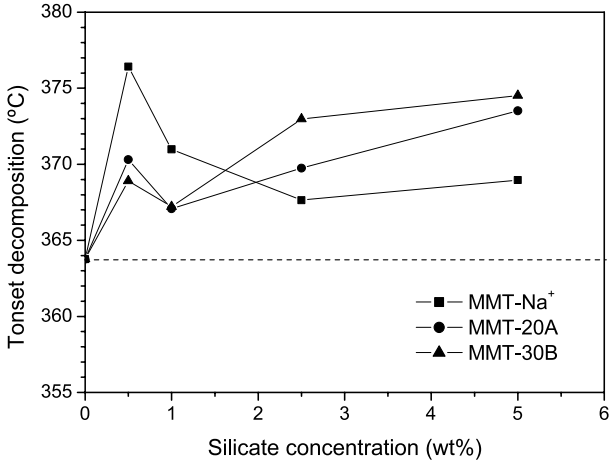

Fig. 9. Onset temperatures of the PEO decomposition as a function of the silicate concentration for the various LMW PEO clay nanocomposites.

temperature. The distinct difference in thermal stability between the natural clay and the two organically modified clay nanocomposites can be attributed to the lower intergallery spacing of the Cloisite Na^+ nanocomposites. The influence of clay addition on the thermal stability is often assigned to the increased pathway for the volatile decomposition products [2,27]. A lower intergallery spacing means less intercalated PEO and hence more 'free' (bulk) PEO whose decomposition products can move more freely. This might also explain why a low amount of Cloisite Na^+ has such a positive effect. The organic modifiers present in the modified clays are also subject to thermal degradation, depending on the formed degradation products/ions altering the degradation path of PEO. The actual increase of the decomposition temperature is rather limited when compared to other polymeric nanocomposites [2]. This can be most likely attributed to the difference in actual degradation mechanism of the polymers and the possible specific interactions between PEO and the clay material [27]. The Cloisite 30B nanocomposites display a small additional weight loss at a lower temperature which is not seen for the other clay nanocomposites and can most likely be attributed to a decomposition of the organic modifier present in Cloisite 30B.

4. Conclusions

PEO nanocomposites based on various clay types of the Cloisite range were prepared according to a melt mixing procedure. The structural organisation and the resulting mechanical properties were found to be very dependent on the matrix molar mass, the clay modifier and the clay concentration. PEO/Cloisite Na^+ nanocomposites gave rise to intercalated nanostructures with a basal spacing increase of 6.5 Å, regardless of the clay concentration and the matrix molar mass. Their mechanical properties showed only a very moderate enhancement at higher clay concentrations.

The use of organically modified clays proved to be essential in order to achieve sufficiently improved mechanical properties. The actual chemical structure of the organic modifier and the matrix molar mass both play a crucial role. The nanocomposites based on Cloisite 30B, containing a polar modifier, displayed exfoliated nanostructures with highly improved storage moduli which increased with increasing clay content, regardless of the matrix molar mass. The obvious compatibility of the modifier and PEO can be held responsible for the obtained nanostructure. On the other hand, the nanostructure of the nanocomposites based on Cloisite 20A, containing an apolar modifier is found to be very dependent on the matrix molar mass. A high PEO molar mass, and thus corresponding high melt viscosity, is needed to obtain exfoliated structures leading to highly improved mechanical properties. In general, it can be stated that the nanocomposites having an exfoliated structure and a high matrix molar mass, displayed the best mechanical properties. The thermal characteristics of the PEO matrix were also found to be influenced by the addition of clay. This effect is, however, less dependent on the resulting nanostructure. Overall, it could be seen that the melt temperature and the overall crystallinity decreased upon the addition of clay. The organically modified clays displayed the strongest effect, especially for the lower molar mass PEO nanocomposites. The onset of the decomposition temperature was found to be slightly increased upon the addition of clay. A minor clay concentration is already very effective. The organically modified clays display the strongest increase of the decomposition temperature.

Acknowledgements

The authors wish to thank Katarina Flodström of the Department of Physical Chemistry 1 of Lunds University for the use of the SAXS apparatus, as well as for the guidance and discussions.

References

[1] Vaia RA, Giannelis EP. MRS Bull 2001;6:394–400.
[2] Alexandre M, Dubois P. Mater Sci Eng 2000;28:1–63.
[3] Van Es M. PhD thesis, TUDelft, The Netherlands, 2001.
[4] Fornes TD, Paul DR. Polymer 2003;44:3945–61.
[5] Jacob MME, Hackett E, Giannelis EP. J Mater Chem 2003;13:1–5.
[6] Aranda P, Ruiz-Hitzky E. Acta Polym 1994;45:59–67.
[7] Sandi G, Joachin H, Kizilel R, Seifert S, Carrado KA. Chem Mater 2003;15:838–43.
[8] Doeff M, Reed JS. Solid State Ionics 1998;113–115:109–15.
[9] Chen H-W, Chang F-C. Polymer 2001;42:9763–9.
[10] Vaia RA, Vasudevan S, Kraweic W, Scanlon LG, Giannelis EP. Adv Mater 1995;7:154–6.
[11] Wen Z, Gu Z, Itoh T, Lin Z, Yamamoto O. J Power Sources 2003; 119–121:427–31.
[12] Chen W, Xu Q, Yuan RZ. Mater Sci Eng B 2000;77:15–18.
[13] Strawhecker KE, Manias E. Chem Mater 2003;15:844–9.
[14] Kwiatkowski J, Whittaker AK. J Polym Sci: Part B: Polym Phys 2001; 39:1678–85.
[15] Hackett E, Manias E, Giannelis EP. Chem Mater 2000;12:2161–7.
[16] Chaiko DJ. Chem Mater 2003;5:1105–10.
[17] Riley M, Fedkiw PS, Khan SA. J Electrochem Soc 2002;149: A667–A74.
[18] Dennis HR, Hunter DL, Chang D, Kim S, White JL, Cho JW, Paul DR. Polymer 2001;42:9513–22.
[19] Vaia RA, Giannelis EP. Macromolecules 1997;30:8000–9.
[20] Lepoittevin B, Devalckenaere M, Pantoustier N, Alexandre M, Kubies D, Calberg C, Jerome R, Dubois P. Polymer 2002;43:4017–23.
[21] Fornes TD, Yoon PJ, Keskkula H, Paul DR. Polymer 2001;42: 9929–40.
[22] Nielsen NE. Mechanical properties of polymers and composites. vol. 2. New York: Marcel Dekker Inc.; 1974. Chapter 8.
[23] Boyd RH. Polymer 1985;26:323–47.
[24] Boyd RH. Polymer 1985;26:1123–33.
[25] Ogata N, Kawakage S, Ogihara T. Polymer 1997;38:5115–8.
[26] Edman L, Ferry A, Doeff MM. J Mater Res 2000;15:1950–4.
[27] Zhao Q, Samulski ET. Macromolecules 2003;36:6967–9.